PHYSICAL REVIEW B **84**, 041306(R) (2011)

Model system for controlling strain in silicon at the atomic scale

Philipp Studer,[1,2] Steven R. Schofield,[1,3] Greg Lever,[3] David R. Bowler,[1,3] Cyrus F. Hirjibehedin,[1,3,4] and Neil J. Curson[1,2]
[1]*London Centre for Nanotechnology, UCL, London, WC1H 0AH, United Kingdom*
[2]*Department of Electronic and Electrical Engineering, UCL, London, WC1E 7JE, United Kingdom*
[3]*Department of Physics and Astronomy, UCL, London, WC1E 6BT, United Kingdom*
[4]*Department of Chemistry, UCL, London, WC1H 0AJ, United Kingdom*
(Received 1 June 2011; published 22 July 2011)

Strain induced by antiphase boundaries (APBs) in the Si(111)2 × 1 surface is investigated using scanning tunneling microscopy (STM), laterally resolved scanning tunneling spectroscopy (STS), and density functional theory (DFT). We determine the structure of all identified APB reconstructions and show that a band shift of states close to the Fermi energy leads to the previously observed electronic contrast. The orientation of the band shift and the observed movement of APBs within the surface are explained by surface strain resulting from the excess free energy of the boundary. We demonstrate that the location of APBs and their associated strain can be precisely manipulated, making them an ideal model system to study and control strain at the atomic scale.

DOI: 10.1103/PhysRevB.84.041306 PACS number(s): 68.35.Gy, 68.35.bg, 68.37.Ef, 73.20.At

The ever decreasing size of semiconductor devices has reached the point where their functionality can rely on only a few atoms.[1] Precise control over the surrounding environment of such devices is important because the presence of atomic-scale defects can have a detrimental influence on the device functionality and limit the achievable scaling. Recently, the understanding of surface defects has improved such that many of them can now not only be avoided but can actually be controlled at the atomic scale. This enables the deliberate arrangement of surface defects such as step edges and vacancies[2,3] to modify the nanoscale properties of the semiconductor. Spatial control over defects thus allows us to harness their specific characteristics and employ them to create novel device structures or study new physics.[4,5]

Future nanoscale semiconductor devices are likely to be strongly influenced by strain because controlling strain enables the engineering of structural, optical, and electronic characteristics such as crystal-field splitting,[6] absorption-band shifts,[7] and piezoresistance.[8] However, measuring and especially controlling strain on the atomic scale remains a great challenge.[9] Defects may provide an elegant solution to study and control strain at the atomic level if suitable structures can be found and control mechanisms established. Antiphase boundaries (APBs) in silicon are promising candidates because crystal boundaries are generally associated with strain[10] and APBs in the Si(111)2 × 1 surface are mobile.[11] Variations in the electronic structure at the surface have been observed around APBs,[11] but the origins of this phenomenon, as well as the atomic structure of the boundary and the mechanism for their movement, have remained unclear.

In this work we show that APBs in the Si(111)2 × 1 surface are model systems for studying and controlling strain at the atomic scale. We identify the structure of all observed APB reconstructions and find that the previously observed electronic phenomenon near the boundary originates from a shift of states close to the Fermi energy which we attribute to strain. The movement of APBs and the origin of the strain are explained in terms of free surface energy reduction. Finally, we show that the location of APBs and their associated strain can be manipulated in a controlled way using the STM tip.

Experiments were performed in an Omicron LT-STM with a base pressure below 5×10^{-11} mbar. Samples were cut from a phosphorus-doped (211) wafer with a resistivity of 0.1–10 Ω cm. To expose the (111) surface, samples were cleaved in situ at room temperature, loaded into the STM at 77 K, and subsequently heated to 200 K where the sample conductivity was suitable for measurements.

Upon cleaving, the Si(111)2 × 1 surface reconstruction is formed as shown in Fig. 1(a), which is described by the Pandey model.[12,13] APBs are created when two domains meet that have π-bonded chains with the same orientation but shifted by half a unit cell in the $[2\bar{1}\bar{1}]$ direction. By studying over sixty APBs on different samples, we found that they can be classified into the three different reconstructions shown in Figs. 1(b)–1(d), denoted as APB1–APB3, respectively. Approximately 80% of all boundaries were APB1 reconstructed whereas APB2 and APB3 each accounted for about 10%.

To determine the structure of APBs, the buckling orientation of atoms in the π-bonded chains has to be considered. As shown in Fig. 1(a) the bias voltage (sample bias convention) can be chosen to selectively image the up- or down-buckled atoms.[14] If the buckling changes over an APB, the up atoms have to align over the boundary in the $[2\bar{1}\bar{1}]$ direction,[15] which is indicated by a white line in Figs. 1(b) and 1(c). It can be seen that the atoms are out of phase across the boundaries, demonstrating that the buckling does not change. We have not encountered any APBs where the buckling changes. Therefore, in agreement with the literature for low-n-type-doped silicon,[16] we conclude that our surface is entirely positively buckled, as shown in Fig. 1(e).

Based on high-resolution STM measurements we have developed atomic structure models for all APB reconstructions shown in Figs. 1(f)–1(h). A model similar to APB2 was previously suggested for APBs observed in Ge(111)2 × 1.[17] APB1 and APB2 follow the equivalent $[1\bar{1}0]$ and $[10\bar{1}]$ direction, respectively, but are not identical because the buckling breaks the surface symmetry. The overlay of the structural model and the STM data show excellent agreement for all reconstructions, as displayed in Figs. 1(b)–1(d). We note that, for APB3, an alternative structure where all π-bonded

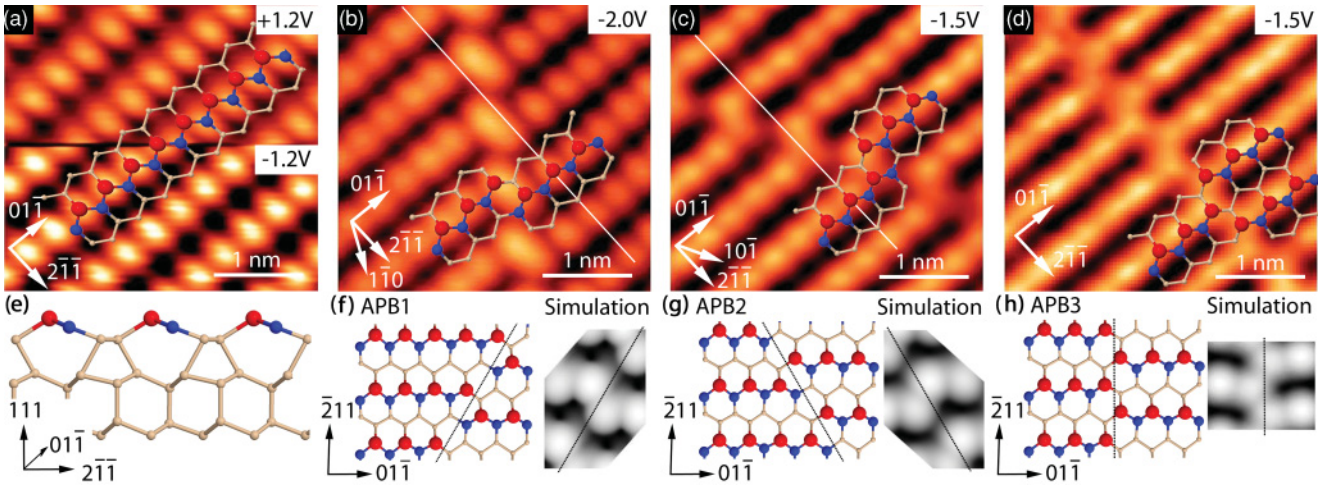

FIG. 1. (Color online) (a) Si(111)2 × 1 surface measured with different bias polarity. (b)–(d) APB reconstructions are shown with an overlay of their atomic structure. (e) Model of the positive-buckled Pandey reconstruction. (f)–(h) The atomic structure of the three APB reconstructions of (b)–(d) respectively, together with their simulated Tersoff-Hamann images for a bias of −1.1 V.

chains terminate in a down-buckled atom does not match the measured corrugation.

Density functional theory (DFT) calculations of the APB structures were performed using VASP[18] with the PW91 GGA[19] functional. A ten-layer Si slab (320 atoms) was used, with the top eight layers free to move and the bottom terminated with H (32 atoms). Cells had to contain several APBs to satisfy the periodic boundary conditions. All forces were converged to within 0.03 eV/Å, and total energies are normalized as energy per boundary between two individual π-bonded chains. For APB1 and APB2, the calculated formation energies were found to be 0.30 eV and 0.34 eV, respectively. Simulated STM images, in Figs. 1(f) and 1(g), show excellent agreement with the measurement, reproducing the central kink with the correct orientation. The energy of APB3 could not be determined because, while one of the two boundaries in the cell converged to the proposed structure shown in Fig. 1(d), the other APB converged to a boundary with π-bonded chains terminated in a down-buckled atom. Future work using larger cells will clarify why the two boundaries converged differently and determine the energy of APB3. As seen in Fig. 1(h) the simulated image of the proposed APB3 structure matches the topography, reproducing the zigzag chain, while the image with down-buckled atoms (not shown) does not. This supports the experimental assignment of the structural overlay shown in Fig. 1(d).

We found that the reported contrast around APBs[11] is bias dependent and strongly asymmetric. As seen in Fig. 2(a), both domains to either side of the APB appear identical when imaged at high bias voltages, whereas they become bright and dark, respectively, when imaged at low bias. The fact that the contrast reverses with voltage polarity demonstrates the electronic nature of this effect.

The electronic contrast was always found to increase the brightness to one side and decrease it to the other side of the APB, giving it a clear orientation. Surprisingly we observed APBs of identical reconstruction type with opposite sides of increased and decreased brightness, respectively, as shown in Figs. 2(a) and 2(b). We found that all three APB reconstructions show the electronic effect in both orientations with about equal distribution. As mentioned before, different buckling on either side of the APB can be excluded. It is therefore evident that the electronic contrast cannot result from local structural aspects of the boundary and that its orientation must be determined by external factors.

In Fig. 2(c) we show the laterally resolved differential conductance at −1.1 V. To visualize the local density of states across the boundary, all spectra of a single π-bonded chain

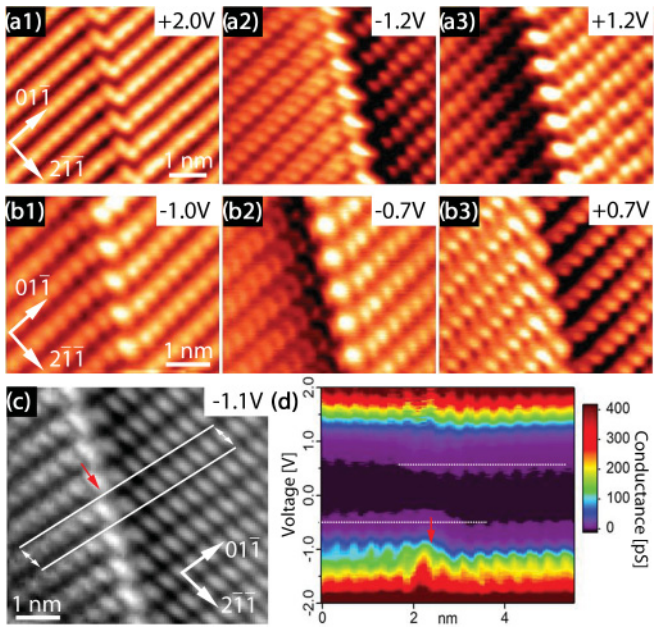

FIG. 2. (Color online) (a1)–(a3) and (b1)–(b3): Two APBs with identical reconstruction but opposite orientation of the electronic effect. (c) Laterally resolved differential conductance. (d) Differential conductance cross section generated by averaging the spectra between the white lines in (c). The arrow marks the position of the APB in both (c) and (d). STS was acquired at −2 V, 300 pA. The spectral resolution after topography correction and smoothing is 80 mV.

were averaged along the $[2\bar{1}\bar{1}]$ direction and are shown in Fig. 2(d). The Fermi level for Si(111)2 × 1 is pinned at +0.4 V due to the surface states.[20] It can be seen that the measured contrast originates from states close to the Fermi level which are shifted by about 200 meV in opposite directions to either side of the boundary. When going further away in energy from the Fermi level, the band shift is reduced and, at ±2 V, it has almost completely disappeared, in good agreement with the voltage-dependent topography measurements. The electronic effect also gradually decreases when laterally moving away from the boundary and disappears after 5 nm.

To determine the cause of the electronic effect, the ability of APBs to move within the surface has to be considered. We frequently observed boundaries relocating over a distance of several nanometers, as shown in Figs. 3(a)–3(c). The movement itself happens between individual line scans, too quickly to be resolved in our measurement. This is shown in Fig. 3(b) where the APB is imaged in four different positions, indicated by the numbered arrows.

It is surprising that APBs are able to move because relocating a boundary requires the breaking of Si bonds. However, we are able to suggest a low-energy pathway for movement based on an earlier calculation by Northrup *et al.*[21] To shift the APB by one unit cell the seven and five atomic rings of the Pandey reconstruction have to swap places. A possible mechanism is to first transform the seven and five atomic rings to a row of six atomic rings and then back to the Pandey model with opposite phase as shown in Fig. 3(e). This requires breaking two bonds per π-bonded chain. We found that these are the same bonds that have to be broken when forming the Pandey model from the buckled reconstruction and the energy barrier to do so was calculated to be less than 100 meV per surface atom.[21] A mechanism where atoms closest to the boundary transform to the buckled reconstruction and then to the Si(111)2 × 1 with opposite phase therefore enables the boundary to move by twice overcoming a barrier of 100 meV per surface atom. However, it is important to keep in mind

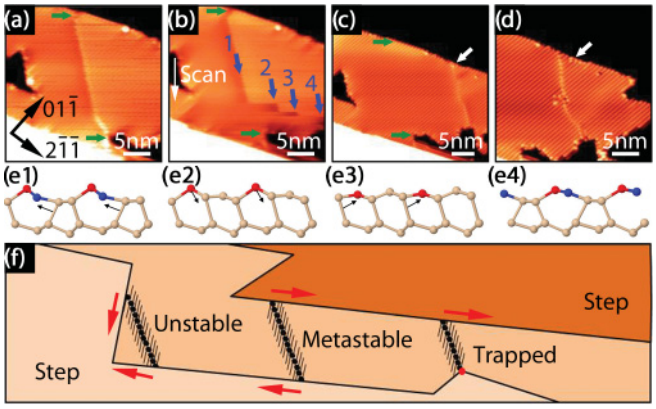

FIG. 3. (Color online) (a) APB imaged in its original position, marked by green (gray) arrows. (b) Movement of the APB to the right in 4 discrete steps. (c) End position after the movement where the APB remained, marked by a white arrow (d). Artificially introduced defect pinning the APB in a new location. (e) Proposed reconstruction mechanism for the movement. (f) Schematic of different possible environments for APBs.

that a boundary between two π-bonded chains cannot move completely independent of its neighbors. This would lead to the formation of two π-bonded chains or troughs next to each other and increase the total energy of the system. Therefore, provided enough (thermal) energy exists to overcome the very small 100 meV barrier, the entire APB has the ability to freely move across the surface as long as no part of it is restrained.

The fact that APBs have a higher energy than the clean surface makes it energetically favorable to eliminate them. Because a boundary has the possibility to change in length by relocating on the surface, as shown in Fig. 3(f), its free energy acts as a driving force[22] to move it in a direction where it becomes shorter. The potential landscape in which an APB moves is therefore defined by the local environment of its end points since they determine how its length is affected by any movement, as sketched in Fig. 3(f). In unstable environments both ends can reduce the length of the APB and therefore minimize its free energy by propagating in the same direction. The boundary shown in a trapped environment, on the other hand, cannot move without increasing its free energy and is therefore pinned. The APB shown in a metastable environment can move without changing in length and would likely diffuse across the surface until it reaches a trapped state or an atomic-scale defect that pins one of its ends. We propose that, after the cleave, all unstable APBs propagate through the surface until they vanish or are pinned, in good agreement with the fact that all boundaries were found in either a trapped or a metastable position. APBs in metastable environments were observed to readily relocate during imaging, confirming their weak local pinning. The movement shown in Fig. 3 can be explained with this model. Tip-induced forces, which will be discussed later, release the APB from its pinned position and allow it to move into the next local energy minima, as shown in Fig. 3(c).

Pinned APBs are prevented from moving at one end and their path across the surface is restricted to the orientations of the three different reconstructions. Defined by the environment of their unpinned side, they are still subjected to a potential gradient, leading to a force acting on the boundary. Because the pinning prevents any movement, this force results in compressive or tensile strain to either side of the APB, depending on its direction. This is in good agreement with the observed characteristics of APBs, because strain is known to induce an electronic contrast in silicon[23,24] and can shift bands in both directions depending on whether it is tensile or compressive.[25] We therefore interpret the electronic contrast as a strain-induced band shift in the Si(111)2 × 1 reconstruction.

Further evidence linking the measured band shift to strain is the observed correlation to the movement of APBs. In Fig. 4 an APB is shown that changes its reconstruction from APB1 to APB3 along its length across the surface. The electronic effect is clearly evident at low bias, and it can be seen that its orientation changes together with the reconstruction. In terms of surface strain this can be explained by two APBs that both try to reduce their length, pulling in opposite directions and forming a delicate balance. In Fig. 4(f) it can be seen that the APB dislocates when imaged at high negative bias, and it is assumed that tip-induced forces disturb the balance between the two boundaries. This is in good agreement with the observation that the movement originates directly at the

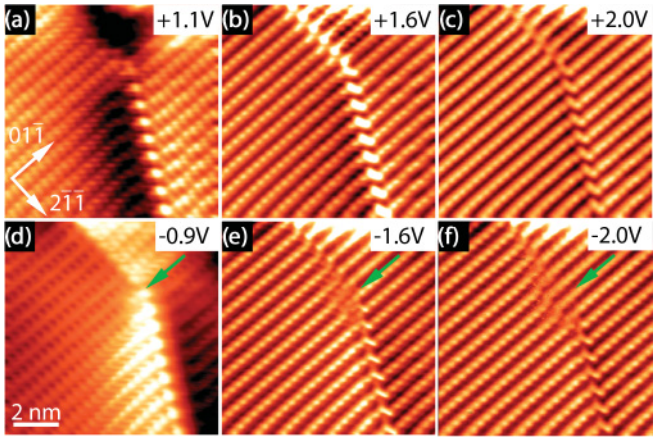

FIG. 4. (Color online) Voltage-dependent imaging of an APB acquired with a current setpoint of 300 pA. The arrow indicates the same position on the surface.

crossover of the two reconstructions, where the electronic contrast changes its polarity.

The change in location was found to increase gradually with increasing negative voltage, demonstrating the influence of the tip. Figures 4(c) and 4(f) were acquired on the forward and backward trace, respectively, of the same scan, illustrating that the switching in between the two positions is very fast and completely reversible. The difference in tip height for both images was measured to be less than 2 pm and, because the boundary only moves under negative voltage, we can exclude tip proximity as the driving mechanism. We assume that either the electric field[26] or a vibrational excitation[27] mediates the movement; further work is required to clarify the exact mechanism.

The ability of the STM to introduce atomic-scale defects combined with the mobility of APBs allows one to accurately control their position. As shown in Fig. 3, APBs can be released through tip-induced forces and will propagate across the surface until they reach the next naturally formed energy minima. Because STM tips can be used to deliberately create defects in silicon,[28] it is possible to control the position of APBs by introducing new pinning sites, as shown in Fig. 3(d). It can be seen that the APB changes its location and now runs through the artificially created defect. APBs that are pinned in a small local energy minima can therefore be released using the tip and then stopped at any desired location using a previously created artificial pinning site.

In summary, we show that APBs are a model system for studying and manipulating the influence of strain at the atomic scale. This enables the exciting possibility of using strain to influence and control the properties of individual atomic-scale devices. Possible applications range from controlling the inhomogeneous broadening of dopants for optical quantum computing[29] to modifying the magnetocrystalline anisotropy of individual atoms for high-density data storage.[30] The atomic model of the boundaries presented here and the detailed data about their band structure will also allow further calculations to determine the forces involved in APB movement and the magnitude of the strain resulting from their pinning.

We acknowledge J. K. Garleff, C. Çelebi, P. M. Koenraad, A. M. Stoneham and G. Aeppli for stimulating discussions. This work was supported by EPSRC EP/D063329/1 and EP/H003991/1.

[1] M. Fuechsle, S. Mahapatra, F. A. Zwanenburg, M. Friesen, M. A. Eriksson, and M. Y. Simmons, Nature Nanotechnol. **5**, 502 (2010).
[2] T. Ogino, H. Hibino, and Y. Homma, Appl. Surf. Sci. **117-118**, 642 (1997).
[3] J. W. Lyding, T. C. Shen, J. S. Hubacek, J. R. Tucker, and G. C. Abeln, Appl. Phys. Lett. **64**, 2010 (1994).
[4] P. G. Piva, G. A. DiLabio, J. L. Pitters, J. Zikovsky, M. Rezeq, S. Dogel, W. A. Hofer, and R. A. Wolkow, Nature (London) **435**, 658 (2005).
[5] D. H. Lee and J. A. Gupta, Science **330**, 1807 (2010).
[6] R. S. Jacobsen, K. N. Andersen, P. I. Borel, J. Fage-Pedersen, L. H. Frandsen, O. Hansen, M. Kristensen, A. V. Lavrinenko, G. Moulin, H. Ou, C. Peucheret, B. Zsigri, and A. Bjarklev, Nature (London) **441**, 199 (2006).
[7] A. M. Smith, A. M. Mohs, and S. Nie, Nature Nanotechnol. **4**, 56 (2009).
[8] Y. Yang and X. Li, Nanotechnology **22**, 015501 (2011).
[9] M. Hytch, F. Houdellier, F. Hue, and E. Snoeck, Nature (London) **453**, 1086 (2008).
[10] I. Rychetsky, J. Phys. Condens. Matter **9**, 4583 (1997).
[11] T. Trappmann, C. Sürgers, and H. v. Löhneysen, Appl. Phys. A **68**, 167 (1998).
[12] K. C. Pandey, Phys. Rev. Lett. **47**, 1913 (1981).
[13] J. K. Garleff, M. Wenderoth, K. Sauthoff, R. G. Ulbrich, and M. Rohlfing, Phys. Rev. B **70**, 245424 (2004).
[14] J. A. Stroscio, R. M. Feenstra, and A. P. Fein, Phys. Rev. Lett. **57**, 2579 (1986).
[15] H. Hirayama, N. Sugihara, and K. Takayanagi, Phys. Rev. B **62**, 6900 (2000).
[16] G. Bussetti, B. Bonanni, S. Cirilli, A. Violante, M. Russo, C. Goletti, P. Chiaradia, O. Pulci, M. Palummo, R. Del Sole, P. Gargiani, M. G. Betti, C. Mariani, R. M. Feenstra, G. Meyer, and K. H. Rieder, Phys. Rev. Lett. **106**, 067601 (2011).
[17] Y. Einaga, H. Hirayama, and K. Takayanagi, Phys. Rev. B **57**, 15567 (1998).
[18] G. Kresse and J. Furthmüller, Comput. Mater. Sci. **6**, 15 (1996).
[19] J. P. Perdew and Y. Wang, Phys. Rev. B **45**, 13244 (1992).
[20] F. J. Himpsel, G. Hollinger, and R. A. Pollak, Phys. Rev. B **28**, 7014 (1983).
[21] J. E. Northrup and M. L. Cohen, Phys. Rev. Lett. **49**, 1349 (1982).
[22] S. M. Allen and J. W. Cahn, Acta Metall. **27**, 1085 (1979).
[23] J. H. G. Owen, D. R. Bowler, C. M. Goringe, K. Miki, and G. A. D. Briggs, Surf. Sci. **341**, L1042 (1995).

[24]S. R. Schofield, N. J. Curson, J. L. O'Brien, M. Y. Simmons, R. G. Clark, N. A. Marks, H. F. Wilson, G. W. Brown, and M. E. Hawley, Phys. Rev. B **69**, 085312 (2004).

[25]Z. Wu, J. B. Neaton, and J. C. Grossman, Nano Lett. **9**, 2418 (2009).

[26]W. G. Schmidt and K. Seino, Current Applied Physics **6**, 331 (2006).

[27]K. Stokbro, C. Thirstrup, M. Sakurai, U. Quaade, B.-K. Hu, F. Perez-Murano, and F. Grey, Phys. Rev. Lett. **80**, 2618 (1998).

[28]I.-W. Lyo and P. Avouris, Science **253**, 173 (1991).

[29]A. M. Stoneham, A. J. Fisher, and P. T. Greenland, J. Phys. Condens. Matter **15**, L447 (2003).

[30]A. A. Khajetoorians, B. Chilian, J. Wiebe, S. Schuwalow, F. Lechermann, and R. Wiesendanger, Nature (London) **467**, 1084 (2010).